Cell Biochem Biophys (2011) 61:595–603
DOI 10.1007/s12013-011-9242-0

ORIGINAL PAPER

Knockdown of hTERT Alters Biophysical Properties of K562 Cells Resulting in Decreased Migration Rate In Vitro

Yingyu Zhang · Xiaopeng Chen · Xiaofeng Xu · Xianwei Wang · Xifu Wang · Guihong Yuan · Dagong Sun · Weibo Ka · Dongqi He · Zongyao Wen · Weijuan Yao

Published online: 11 August 2011

Abstract It has been shown that 90% of tumors, including hematological malignant tumors and leukemia, have much higher levels of telomerase expression than normal cells. To investigate the effect of telomerase on leukemia cells, we transfected K562, a human erythroleukemia cell line with an antisense-hTERT (human telomerase reverse transcriptase) cDNA vector, and examined the biological and biophysical properties of the stably transfected cells (referred to as KAT). Un-transfected cells (K562) and cells transfected with the empty vector (referred to as KC) were used as controls. Cell growth curve and ^{3}H-TdR test showed that the growth rate and DNA synthesis of KAT decreased compared with those of K562 and KC cells. Apoptosis and cell cycle distribution in KAT cells under normal culture condition were similar to those of K562 and KC cells, but changed after serum deprivation. KAT cells had significantly different biophysical characteristics from K562 and KC in terms of cell electrophoresis, membrane fluidity, membrane fluidity, and viscoelasticity. Furthermore, the transendothelial migration rate of KAT was much lower than those of K562 and KC cells. Confocal microscopy showed that KAT cells had higher F-actin content, suggesting the reorganization of cytoskeleton. Flow cytometry analysis revealed a lowered intracellular calcium concentration and CD71 expression, explaining the high F-actin content in KAT cells. In conclusion, we found that the knockdown of hTERT in K562 cells changed their cytoskeleton and biophysical features, and reduced the cell migration.

Keywords Telomerase · Knockdown · K562 · Biophysics · Migration

Y. Zhang · X. Wang · Z. Wen (✉) · W. Yao (✉)
Hemorheology Center, Peking University Health Science Center, Beijing 100191, People's Republic of China
e-mail: rheol@bjmu.edu.cn

W. Yao
e-mail: weijuanyao@bjmu.edu.cn

Y. Zhang
Institute of Biophysics, Chinese Academy of Sciences, Beijing 100101, People's Republic of China

X. Chen
Chengde Medical College, Chengde 067000, People's Republic of China

X. Xu
Institute of Clinical Laboratory, Beijing TongRen Hospital, Capital Medical University, Beijing 100730, People's Republic of China

X. Wang
Department of Cardiology, Peking University Shougang Hospital, Beijing 100041, People's Republic of China

G. Yuan · D. Sun · W. Ka
Department of Medical Physics, Peking University Health Science Center, Beijing 100191, People's Republic of China

D. He
Department of Biomathematics & Biostatistics, Health Science Center, Peking University, Beijing 100191, People's Republic of China

Introduction

There is evidence that 90% of tumors, including hematological malignant tumors and leukemia, show much higher levels of expression of telomerase than normal cells, thus making telomerase an attractive therapeutic target [1–3, 23]. Emerging anti-telomerase therapies that are currently in clinical trials, might prove useful against some forms of human cancers [2, 3, 8]. Telomerase plays a key role in the maintenance of chromosomal stability by prolonging the telomeres at the end of eukaryotic chromosomes and protecting them from being reduced, during cell proliferation in aging and cancer [4, 5, 7]. Many researchers have studied cellular changes following telomerase knockdown in cancer cells, using either an antisense telomerase expression vector or a dominant-negative hTERT (human telomerase reverse transcriptase) mutant to cause shortening of telomeres [9, 15, 29]. These studies demonstrated that, deletion of telomerase activity maybe involved in triggering cancer cell apoptosis [2, 3, 30]. So, telomerase is an important target for the development of new anticancer drugs and strategies based on the reversal of tumor growth by telomerase inhibition [2, 3].

Most current investigations have focused on the biological and biochemical changes in cancer cells caused by telomerase inhibition, and little is known about their biophysical changes. Some researchers have found that the telomerase activity increased more significantly during the accelerated phase and acute transformation phase than the chronic phase of chronic myelogenous leukemia (CML). CML tumor cells have also been found outside the bone marrow, such as, in the central nervous system, lymph node, and skin [16, 26], suggesting that higher telomerase activity might enhance cancer cell migration in vivo. Previous studies performed in our lab have shown that gene knockdown or overexpression (p53, TFAR19, and TRAIL) might lead to the changes in the biophysical properties of cancer cells, thus modulating their metastasis in vivo [12, 17]. We hypothesize that, the inhibition of telomerase activity may affect the biophysical characteristics of cells. Experimental studies to test this hypothesis, which to our knowledge have not been done, will contribute to our understanding of the role of the elevated telomerase activity in the increased ability of cancer cells to migrate.

In this study, we constructed an antisense-hTERT cDNA vector and transfected it into K562 cells. K562 and K562 transfected with the empty vector pcDNA3.1 were used as controls to assess the effects of telomerase knockdown on the biophysical features and migration of the cancer cells.

Materials and Methods

Cell Line, Construction of Antisense-hTERT Vector, and Transfection

K562 cells were maintained in RPMI1640 with 10% FBS containing 100 U/ml penicillin and 100 mg/ml streptomycin. The plasmid pcDNA3.1 was a kind gift from Prof. Ma Dalong (Department of Immunology, Peking University). The plasmid pLXN-hTERT containing the full-length cDNA of hTERT gene (3.4 kb) was a kind gift from Prof. Shen Fang (Department of Immunology, Peking University). The antisense-hTERT expression vector pcDNA3.1(−)-antisense-hTERT (pAT) was constructed and its sequence was confirmed by sequencing. K562 cells were transfected with pAT by using Lipofectin2000. Geneticin (500–1,000 μg/ml) was added in medium 72 h after transfection. Two weeks later, G418-resistant colonies were isolated and expanded. These cells were referred to as KAT cells. K562 cells and K562 cells transfected with pcDNA3.1(−) were used as negative controls and were referred to as K562 and KC, respectively.

cDNA Preparation and Reverse Transcription-Polymerase Chain Reaction (RT-PCR)

Total RNA was extracted from transfected and un-transfected K562 cells using TRIzol reagent (Invitrogen). One μg of RNA was reverse transcribed using avian myeloblastosis virus (AMV) reverse transcriptase and oligo$(dT)_{15}$ as primer. cDNA was amplified with primers for hTERT. GADPH was used as an internal control. The PCR program for hTERT and GAPDH was as follows: 1 min at 95°C, 1 min at 60°C, 2 min at 72°C, 35 cycles, and a final extension at 72°C for 15 min. Primers were: hTERT (1,493 bp) sense, 5′-GCCTCTTCGACGTCTTCCTA-3′; antisense, 5′-CCCC AATTTGACCCACAG-3′ [16]; GADPH (500 bp) sense, 5′-AAGGTGAAGGTCGGAGTCAACG-3′; antisense, 5′-TGCTAAGCAGTTGGTGGTGCAG-3′ [20]. The PCR products were separated on 1% agarose gel.

Telomerase Concentration Measured by Real-Time Quantitative TRAP Analysis

Telomerase activity was measured by telomere repeat amplification protocol (TRAP) [19]. Cells were lysed in Nonidet P-40 lysis buffer and 100 unit/ml RNase inhibitor (Roche Molecular Biochemicals). For negative control, each sample extract was heat treated at 85°C for 10 min before the telomerase activity assay. Thus, analysis of each sample consists of two assays: one with a test extract and

one with a heat treated extract. The SYBR Green real-time quantitative TRAP assay was conducted with a Quantitative Telomerase Detection (QTD) kit (Allied Biotech Inc., Ijamsville, MD). Twenty-five μl of reaction mixture was prepared by mixing 12.5 μl of 2× QTD premix, 11.5 μl of PCR qualified water, and 1.0 μl of cell extract. About 0.01 μg of protein extract was used for the TRAP assay. The reaction mixture was first incubated at 25°C for 20 min to allow the telomerase in the protein extracts to elongate the TS primer (5′-AATCCGTCGAGCAGAGTT-3′), by adding a TTAGGG-repeat sequence. After that, PCR was performed at 95°C for 10 min followed by 35 cycles of amplification at 95°C for 30 s and 60°C for 30 s, and 72°C for 30 s on a thermo cycler (MJ Research, Waltham, MA). The threshold cycle or C_T value was collected. A standard curve was generated from serial dilutions of telomerase-positive telomerase substrate oligonucleotide (TSR) template (0.5, 0.1, 0.02, 0.004, 0.008, 0.00016, 0.000032, and 0.0000064 μg/ml). The concentration of telomerase (nmol/l) in each specimen was calculated based on the standard curve.

Cell Growth Curve and ^{3}H-TdR Measurement

1×10^5 cells/well were seeded into 24-well plates. Cell numbers were counted for up to 5 days. The cell growth curve was obtained by plotting cell numbers against time. For DNA synthesis measurement, cells (1×10^4 cells per well) were seeded into 96-well plates. [^{3}H]-TdR (Amersham Pharmacia Biotech Inc., Piscataway, NJ) was added to each well at 0.5 mCi/well after 4 ($t = 0$), 24, 48, and 72 h incubation. Radioactivity was determined in a scintillation counter (Wallac1409, Turku, Finland).

Determination of Cell Cycle and Apoptosis

K562, KC, and KAT cells were kept under normal culture condition and deprived of serum for 24 and 48 h. The cells were then collected and their cell cycle distribution, and apoptosis were studied with flow cytometry. 5×10^5 cells were re-suspended in 500 μl PBS and stained with propidium iodide (PI, 50 μg/ml) before being analyzed in flow cytometer.

Measurement of the Cell Electrophoresis Rate

Cells were adjusted to 2×10^6/ml with 9% saccharose/0.9% NaCl solution and sucked into a rectangular tube. The tube was placed in an apparatus (Liang-100, Shanghai Medical University, Shanghai, China) with its two ends embedded into two salt bridges made from agar. The salt bridges were connected to two electrodes. Once the electricity (40 V) was applied, the cells moved toward anode. The movement of the cells can be monitored through microscope with a grid. The time for a cell moving 20 μm was recorded and the electrophoresis rate (μm/s/V/cm) of the sample was calculated by averaging the ten cells [6, 33].

Osmotic Fragility

Osmotic fragility was measured according to the established protocol [14, 35]. In brief, 1×10^5 cells were packed and re-suspended in buffers with osmotic pressures ranging from 0 to 295 mOsm/kg. The cell suspensions were left to equilibrate at room temperature for 1 h and then centrifuged at 200 × g for 5 min. The cell pellet was re-suspended in 100 μl of PBS and the number of intact cells were counted. The percentage of lyzed cells was then calculated. Osmotic fragility curves were obtained by plotting the percentages against osmotic pressures.

Fluorescence Polarization Measurements

2×10^6 cells were incubated at room temperature with 1 μM DPH/PBS for 30 min. The final concentration of the solvent tetrahydrofuran, in which DPH had been predissolved was 0.05%. Cells were resuspended in PBS after washing. Steady-state fluorescence was measured with a fluorescence spectrometer (Hitachi, Japan). The fluorescence polarization parameter p was determined with 360 nm excitation and 430 nm emission wavelength [31]. Measurements were completed within 2–3 h after harvesting. Each experiment was performed at least in triplicate.

Confocal Microscopy (CLSM) Analysis [32]

Cells were fixed in 3.7% formaldehyde/PBS for 10 min at room temperature. After washing in PBS, the cells were resuspended in 0.1% Triton X-100/PBS for 5 min and then incubated in 1% BSA/PBS for 30 min. Cells were labeled with 2 U of rhodamine phalloidin (Molecular Probes) for F-actin and Hochest for nucleus staining for 20 min, and resuspended in PBS. Images were taken from a confocal laser scanning microscope (Leica Lasertechnik, Germany) using a 100× oil lens. The fluorescent intensity was quantified for F-actin signal and DNA content using Image J software.

Flow Cytometry Analysis for Cytoplasm [Ca^{2+}] and Surface Protein CD71

To measure the cytoplasm [Ca^{2+}], 10^6 cells were stained by Fluo-3/AM (Invitrogen, Carlsbad, CA; 10 μmol/l) at 37°C for 40 min and washed before flow cytometry analysis. For CD71, samples were incubated with anti-CD71 mAb (BD Biosciences, San Diego, CA) at 4°C for 1 h. After washing, cells were stained with anti-isotype-specific FITC-conjugated IgG (Santa Cruz Biotech., Santa Cruz,

CA). After washing, the samples were run on a FAC Scan (Becton–Dickinson, Mountain View, CA), gated to exclude cell debris and nonviable cells. At least 10,000 events/sample were analyzed. The results were expressed as the difference between the mean fluorescence intensities of the experimental group and the control group.

Elastic and Viscous Moduli of Cells Determined by Micropipette Aspiration System

The micropipette aspiration system was used to determine the elastic and viscous moduli of K562, KC, and KAT cells following the established protocol [12, 31]. In brief, a negative pressure was applied to the micropipette to aspirate a small portion of the cell into micropipette. The time course of cell deformation was continuously recorded on the video recorder. The length of the cell tongue aspirated into the micropipette was determined as a function of time. A standard solid viscoelastic model was used to fit the experimental data. Elastic moduli, K_1 and K_2, and viscous modulus, μ, were calculated.

Cell Migration in Transwell [16]

Human umbilic vascular endothelial cells (HUVECs) were seeded onto the upper compartment surface of the microporous membrane of a Transwell chamber (5-μm pores; Corning Life Sciences, Edison, NJ). 10^5 cells were added onto the HUVEC monolayers and incubated at 37°C for 12 h. Cells collected from the lower compartment surface of the membrane and in the lower compartment of the solution were counted with a FAC Scan (Becton–Dickinson, Mountain View, CA). The ratio of the cell count in such collected cells to that added to the chamber yields the transendothelial migration percentages of the cells.

Statistical Analysis

Data were presented as means ± standard deviations. The statistical analysis was performed with SPSS 11.5 software. One-way analysis of variance (ANOVA) was performed between multiple groups, and least-significant difference (LSD) post hoc test was used to identify differences within groups. Differences were considered significant when $P < 0.05$.

Results

Knockdown of hTERT in K562 Cells

RT-PCR was performed to detect the hTERT expression in K562 cells transfected with and without antisense-hTERT vector. Figure 1a shows that hTERT expression was not changed by control vector but significantly knocked down by antisense- hTERT. We further quantified the telomerase concentrations in K562, KC, and KAT cells. As shown in Fig. 1b, heat treated samples lost their telomerase activity, and therefore, possess much lower active telomerase concentration than un-heated samples. Among all the un-heated samples, KAT has the lowest active telomerase concentration, suggesting that antisense-hTERT significantly abolished the telomerase concentration.

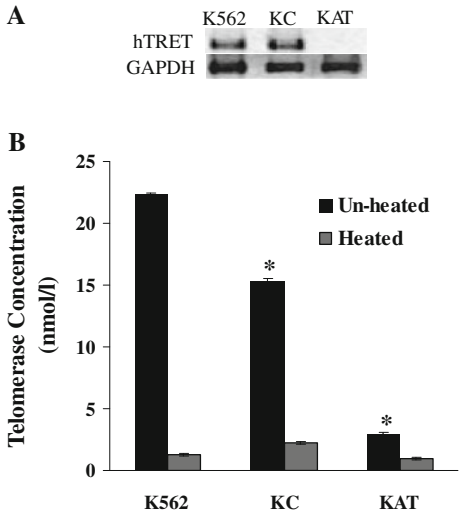

Fig. 1 RT-PCR analysis of hTERT expression and the telomerase concentration as measured by TRAP assay in K562, K562 transfected with control vector (KC), and K562 transfected with antisense-hTERT vector (KAT). **a** Electrophoresis gel pictures for hTRET and GAPDH PCR products. **b** Telomerase concentration (nmol/l) for heated and un-heated cell lysates

The Changes in Cell Growth, DNA Synthesis, Apoptosis, and Cell Cycle Distribution Induced by Knockdown of hTERT

We first examined the biological effects of hTERT knockdown. Cell growth rate, DNA synthesis, apoptosis, and cell cycle distribution of K562, KC, and KAT cells were determined. The cell counting result (Fig. 2a) shows that the growth rate of KAT cells was significantly slower compared with KC and K562 cells ($P < 0.01$). ^{3}H-TdR assay (Fig. 2b) indicates that the DNA synthesis rate of KAT cells after 24, 48, and 72 h culture was significantly lower than those of KC and K562 cells ($P < 0.01$). The apoptosis was analyzed by flow cytometry under three culture conditions, i.e., normal condition, with serum deprivation for 24 and 48 h. Figure 2c shows that, after 24 and 48 h of serum deprivation, the percentage of apoptotic cell in KAT rose dramatically and was much higher than those of K562 and KC ($P < 0.05$). We further found that

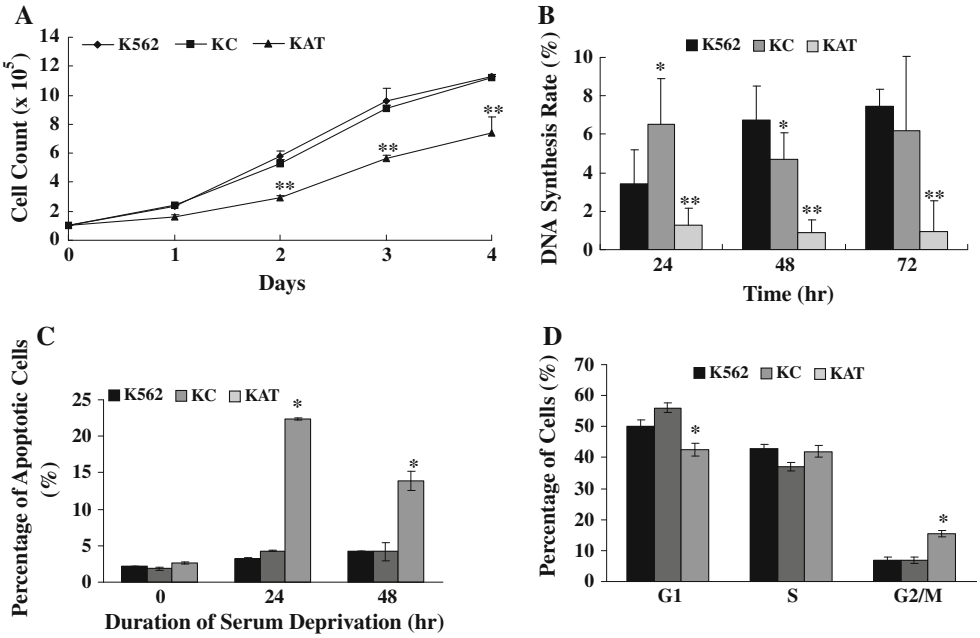

Fig. 2 Cell growth, apoptosis, and cell cycle distribution in K562, K562 transfected with control vector (KC), and K562 transfected with antisense-hTERT vector (KAT). **a** Cell growth curve. **b** Cellular DNA synthesis rate measured by ^{3}H-TdR incorporation for 24, 48, and 72 h. **c** Apoptosis analysis on the cell cultured under normal condition and serum deprivation condition for 24 and 48 h. **d** Cell cycle distribution in G1, S, and G2/M phases for the cells cultured in serum deprivation for 48 h. $^{*}P < 0.05$; $^{**}P < 0.01$ as compared to K562 cells

the cell cycle distributions among K562, KC, and KAT cells had no difference under normal condition and serum deprivation for 24 h (data not shown). But after serum deprivation for 48 h, the KAT cells in G1 and G2/M were much less than K562 and KC cells (Fig. 2d).

The Biophysical Changes Induced by Knockdown of hTERT

We then measured the changes of biophysical properties, such as, electrophoretic mobility (EPM), osmotic fragility, and membrane fluorescent polarization, in K562 cells after hTERT knockdown. We found that the EPM of KAT cells was significantly lowered compared with KC and K562 (Fig. 3a). Figure 3b shows that knockdown of hTERT resulted in an increase of fragility in KAT cells determined at different osmolalities, and the percentage of hemolyzed cells in KAT was higher than those in K562 and KC ($P < 0.05$). The fluorescence polarization parameter p, which is inversely related to the microfluidity of the membrane lipid bilayer [24], was higher in KAT than K562 and KC (Fig. 3c), indicating that the knockdown of hTERT reduced the fluidity of K562 membrane. These results indicate that the abilities of KAT to resist hypoosmolality were weaker than K562 and KC, and this might lead to easier damage of KAT when circulating in vivo.

The Changes in Cell Viscoelasticity and Cell Migration Rate Induced by Knockdown of hTERT

To examine the effects of hTERT knockdown on the cell mechanics, we used micropipette aspiration system to measure the viscoelasticity of cells. We found that KAT cells had higher elastic moduli (Fig. 4a), indicating that the KAT cells are less deformable than K562 and KC cells. But there was no significant change in the viscous modulus among the three groups (Fig. 4b). Furthermore, we performed the migration test with Transwell to assess the effects on the cancer cell migration caused by inhibition of hTERT in K562. The result (Fig. 4c) shows that the migration capability of KAT was much lower than those of K562 and KC, indicating that the knockdown of hTERT could decrease K562 migration ability.

The Change in the F-Actin Content after the Knockdown of hTERT

To explain the changes in the cell mechanics, we assessed the F-actin contents in K562, KC, and KAT cells. Cells were stained with rhodamin phalloidin and examined with a confocal microscope. Figure 5a shows representative confocal images of F-actin. Uniform F-actin signals are mainly localized in the membrane of K562 and KC cells,

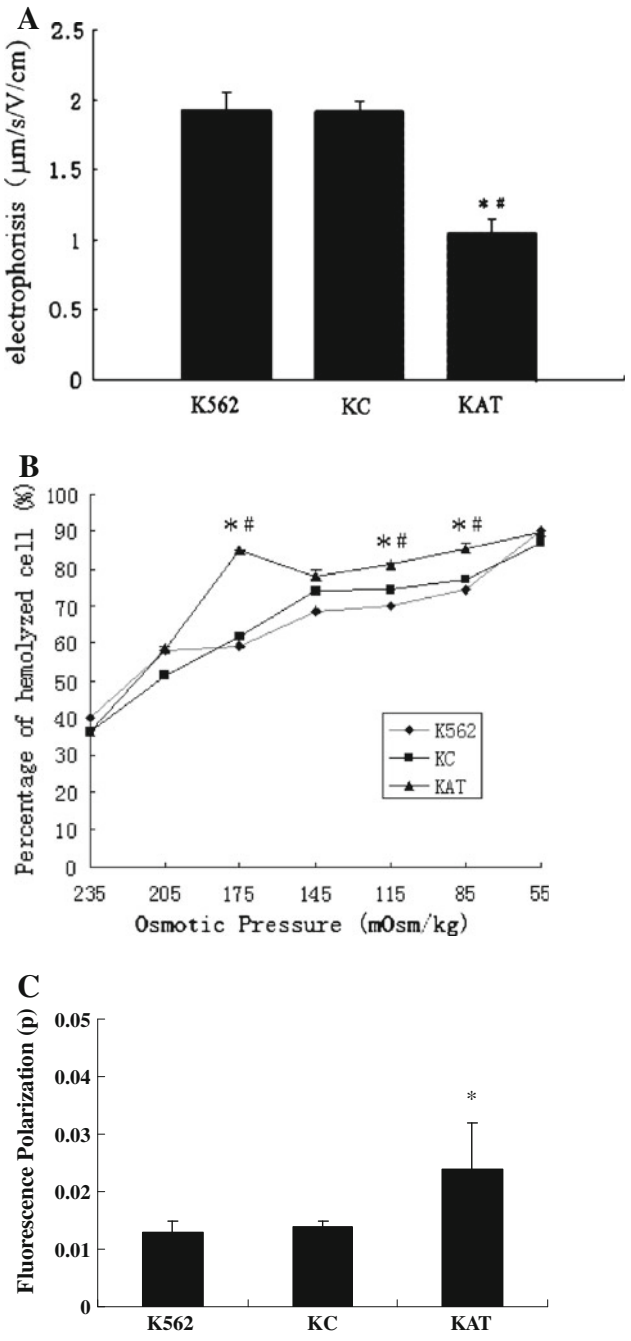

Fig. 3 The biophysical properties of K562, KC, and KAT. **a** Cell electrophoresis rate; **b** the osmolality curve; and **c** the membrane fluidity expressed as the fluorescent polarization (p). $^{*,\ \#}P < 0.05$ as compared with K562 and KC, respectively

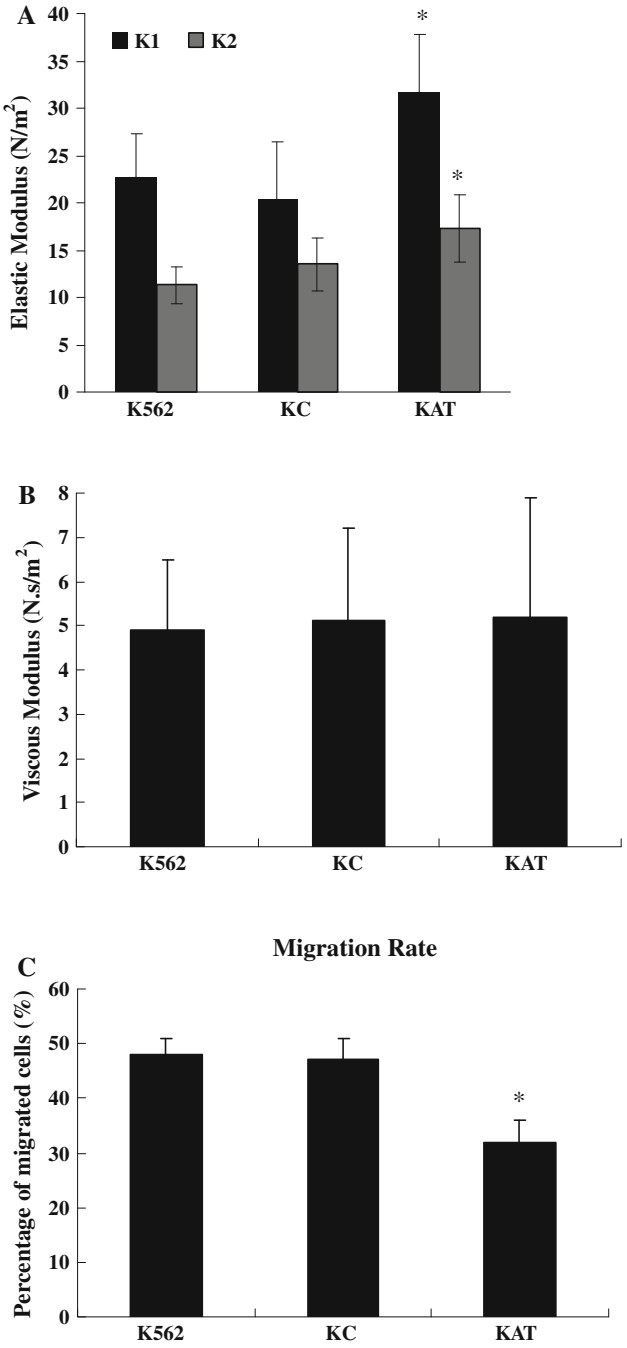

Fig. 4 The viscoelasticity and transendothelial migration of K562, KC, and KAT cells. **a** The elastic moduli, K_1 and K_2; **b** the viscous modulus; and **c** the transendothelial migration rate of the cells. $^{*}P < 0.05$ as compared with K562 cells

but the signals can be found in both the membrane and the cytoplasm of KAT cells, where F-actin aggregates can also be seen. Quantification of images show that the fluorescent intensity of F-actin in KAT was much higher than those of K562 and KC (Fig. 5b), indicating that the knockdown of hTERT resulted in the actin polymerization and reorganization in KAT cells.

Cytoplasm Calcium Concentration and CD71 Expression

We performed flow cytometry to measure the intracellular calcium concentration to elucidate the change of F-actin content in K562 cells with hTERT knockdown. The result shows that the intracellular calcium in KAT cells was much

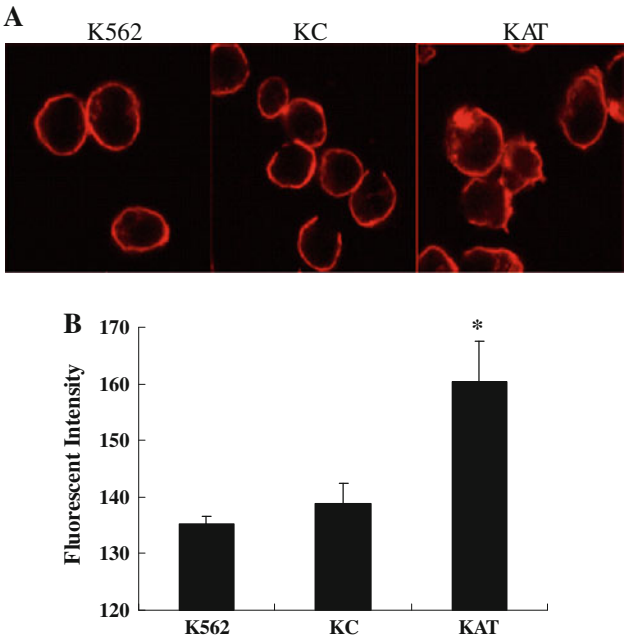

Fig. 5 Confocal microscopy of F-actin and F-actin content. **a** Representative confocal images of rhodamin phalloidin-labeled F-actin in K562, KC, and KAT cells. **b** The fluorescent intensity of F-actin signals quantified from the confocal images. KAT cells had highest intensity among all the three groups. $*P < 0.05$ as compared with K562 cells

lower than K562 and KC cells ($P < 0.05$) (Fig. 6a). To interpret the change of intracellular calcium in KAT cells, we measured the expression level of a surface protein CD71 (Transferrin receptor 1). We found that CD71 expression in KAT cells was much less than those in K562 and KC cells (Fig. 6b).

Discussion

In the present study, we knocked down telomerase in K562 cells by using antisense-hTERT and established the stable antisense-hTERT transfectant KAT. RT-PCR and TRAP assay showed that the expression of hTERT was significantly knocked down in KAT cells. We found that the knockdown of hTERT resulted in the slower cell growth and DNA synthesis rate (Fig. 2a, b), which is consistent with in vivo and in vitro studies [28, 34]. This data indicates that hTERT is involved in the cell growth.

It would be reasonable to speculate that, if the telomerase is knocked down sufficiently, the telomeres would shorten and KAT cells would rapidly begin to crisis. As a result, apoptosis maybe triggered. But interestingly, under normal culture condition, apoptosis was not induced by knockdown of hTERT in KAT cells as compared with K562 or KC cells (Fig. 2c). Consistently, the cell cycle distribution did not change in KAT cells under regular culture condition. But when KAT cells were subjected to serum deprivation for 48 h, significant amount of apoptotic cells appeared, suggesting that the antisense-hTERT may render the K562 cells more vulnerable to stimuli and induce apoptosis. In other words, hTERT may have protective effect on cancer cells.

To test our hypothesis, we characterized the biophysical properties of K562, KC, and KAT cells in terms of cell electrophoresis, osmotic fragility, membrane fluidity, viscoelasticity, and transendothelial migration. Low EPM rate of KAT cells (Fig. 3a) indicated a decrease in the negative potential on the cell surface. It has been shown that the biological properties of tumor cells, such as contact inhibition, infiltration, proliferation, and metastasis, are closely related to surface charges, and EPM of tumor cells is higher than that of normal cells [6]. The decrease in the EPM of KAT indicates that proteins, ligand-receptor binding or other molecular entities on the cell surface are altered, which may signal the cells to undergo apoptosis and inhibit tumor metastasis. High fluorescence polarization parameter p in KAT (Fig. 3c) suggests that the microfluidity of their membrane had decreased, which indicated changes in the composition of membrane. Lower osmotic fragility of KAT than K562 and KC reflects a decrease in the cell's ability to resist lysis (Fig. 3b), suggesting that KAT cells might be more prone to lysis than K562 and KC cells. Micropipette experiments revealed that

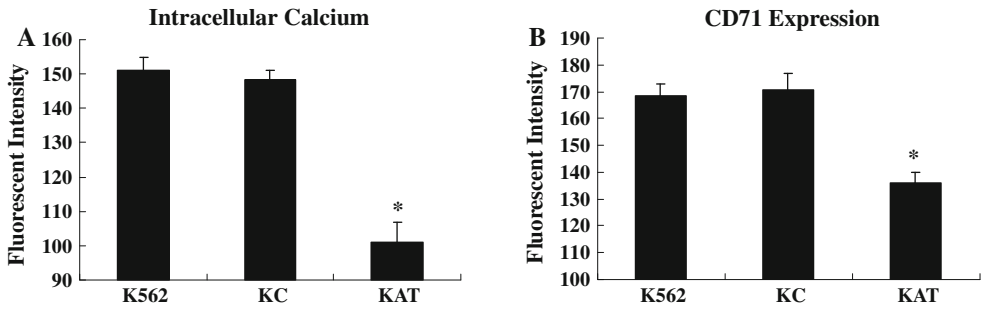

Fig. 6 The measurement of intracellular calcium concentration (**a**) and CD71 expression (**b**) by flow cytometer. $*P < 0.05$ as compared with K562 cells

KAT cells were more rigid than K562 and KC cells (Fig. 4a). These changes may result in the reduced migration in KAT cells as shown in Transwell experiment (Fig. 4c), and facilitate the clearance of KAT in vivo. These results suggest that the introduction of antisense-hTERT into cancer cells might be beneficial for inhibiting their metastasis and facilitating their removal. But it should be pointed out that, the biophysical changes in KAT cells should not be the only reason responsible for their slow migration. There are many reports focused on the biochemical and genetic factors influencing tumor cell migration, such as cell adhesion molecules [22, 27], Cyclophilin A [25], and repression of Socs1 (suppressor of cytokine signaling 1) gene [13], etc. In terms of the mechanistic correlation between our biological data and biophysical measurements, telomerase knockdown in K562 could inhibit its biological function with a decrease in the glucose utilization and phospholipid synthesis. These changes may also provide another reason for the reduced EPM and membrane fluidity in KAT cells [11, 32].

To further explain the biophysical changes caused by hTERT knockdown, we examined the F-actin content by CLSM (Fig. 5) and intracellular calcium concentration, and CD71 expression by flow cytometer (Fig. 6). Compared with those in K562 and KC, F-actin in KAT cells was more in content and more irregular distributed, indicating that the KAT cells had more actin polymerization. The data indicates that the membrane organizations were altered by telomerase knockdown, which may explain the higher viscoelasticity (Figs. 4a, b) and slower migration rate in KAT cells as measured in transwell assay (Fig. 4c). Among the factors that affect the actin polymerization, calcium is of great importance. Calcium participates in regulating the polymerization and organization of actin [10]. The expression of surface protein CD71 is related to the uptake of ions such as Fe^{2+}, Ca^{2+} [18, 21]. We found that the KAT cells had lower intracellular [Ca^{2+}] and CD71 expression than K562 and KC (Fig. 6a, b). This will result in the polymerization of actin in KAT cells and cause the changes in cell viscoelasticity and migration.

In summary, our data have demonstrated the changes in biophysical characteristics in K562 caused by inhibition of telomerase activity. These findings provide direct support for our hypothesis that telomerase activity modulates the biophysical properties of K562 cells. It should be noted that the direct link between the knockdown of hTERT and biophysical changes must be more complex than what we presented. Considering the low cell growth rate in KAT cells, it maybe reasonable that the knockdown of hTERT may cause the cells to enter into the senescent process due to the shortening of telomere and/or the downregulation of the genes. Many signaling pathways in the cells maybe altered and then the biophysical changes are the final consequences. Even though the conclusions got from K562 cells can not be extrapolated to other leukemias or tumor types, these results still help to enhance our understanding of telomerase, and maybe beneficial for tumor gene therapy by using anti-telomerase drugs.

Acknowledgments This study was supported by National Natural Science Foundations of China (Grant No. 10572007 and 30770532). The authors would like to thank University Professor Shu Chien from University of California, San Diego for his valuable suggestions and revisions on the manuscript.

Conflict of interest statement No conflict of interest to disclose.

References

1. Ahmed, A., & Tollefsbol, T. (2003). Telomeres, telomerase, and telomerase inhibition: Clinical implications for cancer. *Journal of the American Geriatrics Society, 51*, 116–122.
2. Akiyama, M., Hideshima, T., Munshi, N. C., & Anderson, K. C. (2002). Telomerase inhibitors as anticancer therapy. *Current Medicinal Chemistry Anticancer Agents, 2*, 567–575.
3. Akiyama, M., Yamada, O., Kanda, N., Akita, S., Kawano, T., Ohno, T., et al. (2002). Telomerase overexpression in K562 leukemia cells protects against apoptosis by serum deprivation and double-stranded DNA break inducing agents, but not against DNA synthesis inhibitors. *Cancer Letters, 178*, 187–197.
4. Blackburn, E. H. (2005). Telomeres and telomerase: Their mechanisms of action and the effects of altering their functions. *FEBS Letters, 579*, 859–862.
5. Blasco, M. A. (2005). Mice with bad ends: Mouse models for the study of telomeres and telomerase in cancer and aging. *EMBO Journal, 24*, 1095–1103.
6. Camp, J. P., & Capitano, A. T. (2005). Size-dependent mobile surface charge model of cell electrophoresis. *Biophysical Chemistry, 113*, 115–122.
7. Counter, C. M., Avilion, A. A., LeFeuvre, C. E., Stewart, N. E., Greider, C. W., Harley, C. B., et al. (1992). Telomere shortening associated with chromosome instability is arrested in immortal cells which express telomerase activity. *EMBO Journal, 11*, 1921–1929.
8. Deng, Y., & Chang, S. (2007). Role of telomeres and telomerase in genomic instability, senescence and cancer. *Laboratory Investigation, 87*, 1071–1076.
9. Dikmen, Z. G., Gellert, Z. G., Jackson, S., Gryaznov, S., Tressler, R., Dogan, P., et al. (2005). In vivo inhibition of lung cancer by GRN163L: A novel human telomerase inhibitor. *Cancer Research, 65*, 7866–7873.
10. Garib, V., Lang, K., Niggemann, B., Zänker, K. S., Brandt, L., & Dittmar, T. (2005). Propofol-induced calcium signalling and actin reorganization within breast carcinoma cells. *European Journal of Anaesthesiology, 22*(8), 609–615.
11. Gu, L., Fang, Y. H., Wang, Y., Yao, W. J., Sun, D. G., Ka, W. B., et al. (2005). TFAR19 gene changes the biophysical properties of murine erythroleukemia cells. *Cell Biochemistry and Biophysics, 43*(3), 355–363.
12. Gu, L., Tang, Z., He, D., Ka, W., Sun, D., & Wen, Z. (2007). Effects of TFAR19 gene on the in vivo biorheological properties and pathogenicity of mouse erythroleukemia cell line MEL. *Science China C. Life Science, 50*, 111–119.
13. Gui, Y., Yeganeh, M., Ramanathan, S., Leblanc, C., Pomerleau, V., Ferbeyre, G., Saucier, C., & Ilangumaran, S. (in press).

SOCS1 controls liver regeneration by regulating HGF signaling in hepatocytes. *Journal of Hepatology*.
14. Guo, J., Zhang, L., Jiang, Y., Zeng, Z., Sun, D., Ka, W., et al. (2005). Effects of Compound Dan-shen Root Dropping Pill on hemorheology in high-fat diet induced hyperlipidemia in dogs. *Clinical Hemorheology Microcirculation, 32*, 19–30.
15. Herbert, B., Pitts, A. E., Baker, S. I., Hamilton, S. E., Wright, W. E., Shay, J. W., et al. (1999). Inhibition of human telomerase in immortal human cells leads to progressive telomere shortening and cell death. *Proceedings of the National Academy of Sciences of the United States of America, 96*, 14276–14281.
16. Iwama, H., Ohyashiki, K., Ohyashiki, J. H., Hayashi, S., Kawakubo, K., Shay, J. W., et al. (1997). The relationship between telomere length and therapy-associated cytogenetic responses in patients with chronic myeloid leukemia. *Cancer, 79*, 1552–1560.
17. Jiang, Y., Chen, K., Tang, Z., Zeng, Z., Yao, W., Sun, D., et al. (2006). TRAIL gene reorganizes the cytoskeleton and decreases the motility of human leukemic Jurkat cells. *Cell Motility and the Cytoskeleton, 63*, 471–482.
18. Kremenetskaia, O. S., Logacheva, N. P., Baryshnikov, A. I., Chumakov, P. M., & Kopnin, B. P. (1996). The effect of the tumor suppressor p53 and its mutant forms on the differentiation and viability of K562 leukemic cells. *Tsitologiia, 38*, 1280–1293.
19. Lee, B. J., Wang, S. G., Choi, J. S., Lee, J. C., Goh, E. K., & Kim, M. G. (2006). The prognostic value of telomerase expression in peripheral blood mononuclear cells of head and neck cancer patients. *American Journal of Clinical Oncology, 29*, 163–167.
20. LeGal, J. M., Morjani, H., Fardel, O., Guillouzo, A., & Manfait, M. (1994). Conformational changes in membrane proteins of multidrug-resistant K562 and primary rat hepatocyte cultures as studied by Fourier transform infrared spectroscopy. *Anticancer Research, 14*, 1541–1548.
21. Liu, M. J., Wang, Z., Ju, Y., Wong, R. N., & Wu, Q. Y. (2005). Diosgenin induces cell cycle arrest and apoptosis in human leukemia K562 cells with the disruption of Ca^{2+} homeostasis. *Cancer Chemotherapy and Pharmacology, 55*, 79–90.
22. Moh, M. C., & Shen, S. (2009). The roles of cell adhesion molecules in tumor suppression and cell migration: A new paradox. *Cell Adhesion and Migration, 3*(4), 334–336.
23. Mu, J., & Wei, L. X. (2002). Telomere and telomerase in oncology. *Cell Research, 12*, 1–7.
24. Nathan, I., Ben-Valid, I., Henzel, R., Masalha, H., Baram, S. N., Dvilansky, A., et al. (1998). Alterations in membrane lipid dynamics of leukemic cells undergoing growth arrest and differentiation: Dependency on the inducing agent. *Experimental Cell Research, 239*, 442–446.
25. Obchoei, S., Wongkhan, S., Wongkham, C., Li, M., Yao, Q., & Chen, C. (2009). Cyclophilin A: Potential functions and therapeutic target for human cancer. *Medical Science Monitor, 15*(11), RA221–RA232.
26. Ohyashiki, K., Ohyashiki, J. H., Iwama, H., Hayashi, S., Shay, J. W., & Toyama, K. (1997). Telomerase activity and cytogenetic changes in chronic myeloid leukemia with disease progression. *Leukemia, 11*, 190–194.
27. Okegawa, T., Li, Y., Pong, R. C., & Hsieh, J. T. (2002). Cell adhesion proteins as tumor suppressors. *Journal of Urology, 167*, 1836–1843.
28. Roth, A., Vercauteren, S., Sutherland, H. J., & Lansdorp, P. M. (2003). Telomerase is limiting the growth of acute myeloid leukemia cells. *Leukemia, 17*, 2410–2417.
29. Wang, E. S., Wu, K., Chin, A. C., Chen-Kiang, S., Pongracz, K., Gryaznov, S., et al. (2004). Telomerase inhibition with an oligonucleotide telomerase template antagonist: In vitro and in vivo studies in multiple myeloma and lymphoma. *Blood, 103*, 258–266.
30. Yamada, O., Akiyama, M., Kawauchi, K., Adachi, T., Yamada, H., Kanda, N., et al. (2003). Overexpression of telomerase confers a survival advantage through suppression of TRF1 gene expression while maintaining differentiation characteristics in K562 cells. *Cell Transplantation, 12*, 365–377.
31. Yao, W., Chen, K., Wang, X., Xie, L., Wen, Z., Yan, Z., et al. (2002). Influence of TRAIL gene on biomechanical properties of the human leukemic cell line, Jurkat. *Journal of Biomechanics, 35*, 1659–1663.
32. Yao, W., Gu, L., Sun, D., Ka, W., Wen, Z., & Chien, S. (2003). Wild type p53 gene causes reorganization of cytoskeleton and, therefore, the impaired deformability and difficult migration of murine erythroleukemia cells. *Cell Motility and the Cytoskeleton, 56*, 1–12.
33. Zeng, Z., Yao, W., Xu, X., Xu, G., Long, J., Wang, X., et al. (2009). Hepatocellular carcinoma cells deteriorate the biophysical properties of dendritic cells. *Cell Biochemistry and Biophysics, 55*, 33–43.
34. Zhang, Y., & He, D. M. (2002). Effect of antisense-hTERT mRNA oligodeoxynucleotide on telomerase activity of leukemic cells. *Cell Biology International, 26*, 427–431.
35. Zhang, Y., Yao, W., Zeng, Z., Wang, X., Sun, D., Ka, W., et al. (2007). Exogenous wild-type p53 gene improved survival of nude mice injected with murine erythroleukemia cell line through amelioration of hemorheological changes. *Microcirculation, 14*, 155–166.